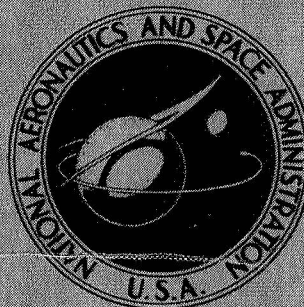


NASA TECHNICAL
MEMORANDUM



NASA TM X-1474

NASA TM X-1474

Declassified by authority of NASA
Classification Change Notices No. 214
Dated 9-30-77

FACILITY FORM 602

N71-74419
(ACCESSION NUMBER) (THRU)
28 (PAGES) none (CODE)
(NASA CR OR TMX OR AD NUMBER) (CATEGORY)

FLIGHT-TEST RESULTS OF AN
X-BAND TELEMETRY SYSTEM
ON A TRAILBLAZER II VEHICLE

by Bruce M. Kendall and Richard F. Harrington

Langley Research Center

Langley Station, Hampton, Va.

UNCLASSIFIED

By Authority of T.O. 70-503, 8-1-71

FLIGHT-TEST RESULTS OF AN X-BAND TELEMETRY SYSTEM ON
A TRAILBLAZER II VEHICLE

By Bruce M. Kendall and Richard F. Harrington

Langley Research Center
Langley Station, Hampton, Va.

NATIONAL AERONAUTICS AND SPACE ADMINISTRATION

FLIGHT-TEST RESULTS OF AN X-BAND TELEMETRY SYSTEM ON
A TRAILBLAZER II VEHICLE *

By Bruce M. Kendall and Richard F. Harrington
Langley Research Center

SUMMARY



The performance of an X-band telemetry system employing pulse-position modulation that was flown aboard a Trailblazer II reentry-research vehicle is discussed. This system was used to investigate the concept of achieving telemetry transmission of data through the reentry period by use of a radiofrequency above the critical frequency of the plasma. The X-band signal was lost for a period of only about 2.4 seconds during the reentry.

INTRODUCTION

Several methods have been proposed for minimizing or eliminating the radio-frequency blackout during atmospheric reentry of a vehicle. (See ref. 1.) Among these, such techniques as addition of material to the flow field or the use of playback tape recorders may not be applicable to small payloads for reentry vehicles because of size, weight, and environmental characteristics. A more applicable method is the use of a telemetry system whose frequency is greater than the critical frequency of the plasma.

On May 4, 1965, the D58-3539 Trailblazer II vehicle was launched from Wallops Island, Virginia, carrying an X-band telemetry system with an operating frequency greater than the plasma critical frequencies normally encountered by the Trailblazer II reentry vehicle. This system was intended to provide the transmission of on-board measurements during the period when a VHF telemetry system would have experienced radio-frequency blackout.

The prime purpose of this and other Trailblazer II flights was to provide a target for radar cross-section measurements. The secondary purpose of the D58-3539 vehicle flight was to obtain reentry research measurements (nose-cap optical radiation, vehicle accelerations, and structure temperatures). The X-band telemetry system was used to transmit these measurements during the reentry period.



It is the purpose of this paper to discuss the performance of the X-band telemetry system on the D58-3539 Trailblazer II vehicle flight.

VEHICLE

The Trailblazer II is a five-stage, solid-propellant, unguided, spin-stabilized vehicle. A photograph of the vehicle and a configuration drawing of the stages are shown in figure 1. The rocket motors are arranged in tandem fashion with the last three stages enclosed in a protective structural shell (velocity package) and facing in a rearward direction at launch. A complete description of this vehicle is contained in reference 2.

The nominal trajectory of the vehicle, shown in figure 2, is obtained as follows: The firing of the first two stages boosts the velocity package along the ascending portion of the trajectory, and the canted fins on the second stage induce the spin stabilization of the vehicle which maintains the velocity-package attitude through the remainder of the flight. Prior to attaining apogee at about 200 statute miles (320 km), the velocity package separates from the second stage. After reaching apogee, the third stage is fired, propelling the reentry stages out of the open end of the velocity package. The motors of the fourth stage and fifth (payload) stage are then fired in succession, driving the payload into the atmosphere to provide the reentry environment for research measurements.

VHF telemetry systems for transmitting data on vehicle performance are located in the nose of the velocity shroud and in the adapter between the third and fourth stages. These systems also provide sources for VHF tracking during the flight prior to fourth-stage ignition.

PAYLOAD

Photographs of the Trailblazer II payload assembled and unassembled are shown in figures 3(a) and 3(b), respectively. Figure 3(c) shows the overall configuration of the payload and the relative placement of the components of the X-band telemetry system. The payload was conical with a 6° half-angle and a 3/4-in. (1.9-cm) nose radius. The frustum of the payload cone was fabricated of aluminum and covered with Avcoat II, a non-charring ablative material. The payload nose was a copper heat sink.

X-BAND TELEMETRY SYSTEM

The X-band telemetry system operated at a frequency of 9210 MHz, employing pulse-position modulation with a data capacity of 900 samples per second. The total system including the antenna and battery pack weighed about 5 pounds (2.3 kg). A functional

[REDACTED]

description of an identical system (with the exception of the magnetron output power) is given in reference 3. The total power consumption of the telemetry system was 33 watts.

Transmitter and Encoder

A photograph of the transmitter and encoder is shown in figure 4(a). The X-band transmitter utilized a magnetron which had a peak output power of 130 watts. A simplified block diagram of the transmitter is shown in figure 4(b). Although limited payload space prevented the use of an isolater between the transmitter and antenna to protect the transmitter magnetron from high VSWR (voltage standing wave ratio) loads, "frequency-pulling" tests conducted on the transmitter indicated a frequency shift of less than 10 MHz for a VSWR change from 1.5:1 to about 10:1. The high VSWR from the antenna mismatch was accomplished by covering the entire antenna aperture with a layer of metallic foil to simulate the worst possible plasma condition. Both the transmitter and the encoder unit were completely solid state with the exception of the transmitter magnetron. The encoder commutated and encoded the sample data to a pulse-position modulation (PPM) format for keying of the X-band transmitter. A simplified block diagram of the encoder is shown in figure 4(c). The inputs to the encoder were 20 low-level differential-input data channels. The sampling rate was 45 times per second, resulting in a total of 900 samples per second. Table I shows the assignment of the 20 data channels in the Trailblazer II payload. Channels 19 and 20 were used to provide a void in the pulse train which was used for frame synchronization in accordance with IRIG (Inter-Range-Instrumentation Group) standards.


Antenna

An antenna was selected to provide omnidirectional coverage in the roll plane of the vehicle within ± 1.5 dB. This antenna consisted of a circular array of 16 slots fed by a waveguide loop which was excited at a single point and shorted 180° from the point of excitation. A photograph of the assembled antenna and a sketch of the design features are shown in figure 5(a). The antenna assembly was an integral part of the payload structure and weighed 14 ounces (0.4 kg).

A sectional view of the antenna mounted in the payload is shown in figure 5(b). A layer of phenolic-nylon dielectric material between the antenna surface and the phenolic-glass laminate and Avcoat II layer assured a minimum dielectric thickness of more than one-quarter wavelength to minimize effects of surface ablation on antenna characteristics. (See ref. 4.) The antenna was located 21.6 inches (54.9 cm) from the nose tip along the longitudinal axis of the payload.

The pitch or yaw radiation pattern for this slot-array antenna mounted in the payload is shown in figure 6(a). However, this radiation pattern existed only after the reentry stages were propelled out of the open end of the velocity shroud by ignition of the third-stage motor. During the initial period of the flight (launch until separation of the second

[REDACTED]



stage from the velocity shroud) the payload was enclosed in the velocity shroud and the X-band signal was propagated through two small circular fiber-glass windows in the shroud. The radiation pattern for this condition is shown in figure 6(b). After separation of the second stage from the velocity shroud, the radiofrequency energy was being radiated out the open end of the shroud with the radiation pattern shown in figure 6(c).

Although it would have been desirable to have utilized directional couplers on the antenna to measure forward and reflected radiofrequency power, limited payload space made this impossible. However, it was possible to insert a sampling probe in the waveguide feed section of the X-band antenna. This probe was fixed in position and measured only the voltage standing wave in the waveguide. Therefore, its output was a function of the forward and reflected radiofrequency power and could vary with amplitude and phase change of the standing wave. However, the probe output provided an indication of the presence of radiofrequency energy in the antenna to show that the X-band transmitter was operating and supplying output power to the antenna.

RANGE INSTRUMENTATION

Figure 7 shows the location of the three X-band receiving systems. Receiving systems 1 and 2 are at Wallops Island, Virginia, and receiving system 3 is at the NASA tracking site at Coquina Beach, North Carolina. Systems 1 and 3 are monopulse trackers with a 1.2° -beam-width circular-polarization antenna, receiver sensitivity of -95 dBm, antenna gain of 36 dB, and overall system sensitivity of -131 dBm. They are described in detail in reference 5. System 2 uses a radar-directed linear-polarization antenna with 0.25° beam width, a receiver sensitivity of -95 dBm, an antenna gain of 52 dB, and an overall system sensitivity of -147 dBm. This system was operated by M.I.T. Lincoln Laboratory.

Acquisition and tracking assistance was provided for the two Wallops Island systems by VHF acquisition trackers and radar trackers. Acquisition for the system at Coquina Beach was provided by a VHF tracker. Systems 1 and 3 also had precalculated antenna-pointing capability.

The approximate tracking signal margins for the worst-case condition of the flight were -3 dB to 9 dB, 13 dB to 25 dB, and 0.5 dB to 15 dB for systems 1, 2, and 3, respectively. These maxima and minima are due to the variation of the payload-antenna pattern with vehicle precession.



RESULTS

Flight Trajectory

The achieved flight trajectory is shown in figures 8, 9, and 10, where altitude as a function of horizontal range, altitude as a function of velocity, and altitude and velocity as a function of flight time are plotted.

Performance of X-Band Telemetry System

Of the three X-band tracking stations, only station 2 (M.I.T.) tracked the payload during the entire flight. Station 1 at Wallops Island experienced acquisition problems and tracked intermittently during the first 50 seconds of the flight. Station 3 at Coquina Beach acquired the payload signal about 60 seconds after launch and tracked for about 123 seconds.

Figure 11 shows a plot of the X-band signal strength received at the antenna of the M.I.T. tracker as a function of flight time. The signal-strength levels shown in this figure are average values obtained by constructing a median line through the fluctuations of the signal-strength (automatic gain control) record of the X-band receiver. These fluctuations were due to the rapid changes in antenna pattern normally encountered on a spinning vehicle. During the first 60 seconds of the flight, the received signal strength was low because the payload was enclosed in the velocity shroud. At about 63 seconds, the second stage separated from the velocity shroud. The large increase in signal strength at this time was caused by the radiofrequency energy then being radiated out the open end of the shroud. This increase in signal strength corresponds directly to an increase in antenna gain, as can be seen in figures 6(a) and 6(b). The gradual decrease in signal strength between 63 and 185 seconds was due to the increase in slant range.

At 185 seconds after launch, an on-board drop in radiofrequency power of 17 dB was experienced, as evidenced by the plot of received signal strength in figure 11 and data from the payload-antenna power monitor. This large decrease in power caused the tracking station at Coquina Beach to lose track, as the signal strength had dropped below the detection level for this station.

From 185 seconds until the time of the firing of the third-stage rocket motor, the signal from the payload was fairly constant, as expected. At about 324 seconds the payload was propelled from the velocity shroud by ignition of the third-stage rocket motor, and the received signal was reduced because of the change from the directional antenna pattern of figure 6(c) to the omnidirectional pattern of figure 6(a). A temporary reduction in received signal occurred at the firing of the fourth- and fifth-stage motors because of momentary acceleration of the vehicle out of the tracking-antenna beam. After the firing

of the fourth- and fifth-stage motors and until the end of the flight, the signal-strength level fluctuated because of antenna-pattern changes caused by precession of the vehicle.


Complete loss of the X-band signal occurred 403.5 seconds after launch, at an altitude of 102 000 ft (31 090 m) and a velocity of 19 500 ft/sec (3514 m/sec). This loss lasted until 405.9 seconds at an altitude of 57 000 ft (17 374 m). After the loss period the signal strength increased above the level prior to this period. The signal was lost at approximately 410 seconds, at which time it is believed that the payload was destroyed. Optical tracking data also confirm this as the time for payload destruction.

Figure 11 shows that after ignition of the third-stage rocket motor a large part of the received signal was below the level (-137 dBm) required by the M.I.T. tracker for proper detection and recording of the received pulses. This low received signal caused a considerable number of missing pulses in the recorded data, and the data had to be reduced manually as the automatic data-reduction system could not distinguish between missing data pulses and missing pulses used for frame synchronization.

Signal-Strength Anomalies

As previously mentioned, the drop in received signal strength 185 seconds after launch was due to a corresponding drop in on-board radiofrequency power as indicated by the telemetry data from the antenna-power monitor. As this time occurred during a period of the flight when there was little environmental effect on the payload, a failure in the on-board radiofrequency transmission line or antenna was unlikely. Voltage breakdown was not a factor in this instance in that during this time the payload was at an altitude far exceeding the critical altitude for voltage breakdown at X-band frequencies, and preflight laboratory tests indicated that breakdown was not a problem for the payload even at the critical altitude. Therefore, the change in monitored radiofrequency power was a change of the forward or transmitted power. Since telemetry data showed that no change occurred in the temperature of the transmitter or antenna-power monitor and that the dc input voltage to the transmitter did not change, the failure was isolated to the transmitter. Laboratory tests were conducted on a magnetron identical to the one in the payload transmitter to simulate the failure condition. As a result of these tests, it was determined that the radiofrequency power reduction was probably due to a drop in the voltage that triggers the magnetron. Such a voltage drop could have been caused by a component failure in the transmitter's power-supply circuit. The fact that the X-band magnetron could have its triggering voltage reduced to such a point that its output power was decreased by 17 dB and still oscillate was an unexpected result.

The complete loss of the X-band signal from 403.5 seconds until 405.9 seconds could have been caused by several factors: (1) radiofrequency voltage breakdown, (2) antenna mismatch, (3) antenna radiation-pattern null, (4) radiofrequency blackout, or (5) tracking



error. The possibility of radiofrequency voltage breakdown has already been discredited. The telemetry data received before and after this period showed that no changes occurred in the temperature of the transmitter or antenna-power monitor and that the dc input voltage to the transmitter did not change. The antenna-power monitor indicated an increase in its output which was probably caused by a mismatch at the antenna. This could have been caused by the presence of a plasma or partial ablation of the Avcoat II material which covers the payload antenna.

A loss of signal of the magnitude experienced during this period could not have been caused by vehicle antenna-pattern null without considerable change in the payload's angle of attack, a condition which the linear (axial) accelerometer did not indicate. The possibility of radiofrequency blackout was very good for this period. Figure 12 shows a velocity-altitude profile which indicates predicted VHF and X-band blackout areas (those areas under each curve) for both an equilibrium far-wake flow condition and a frozen far-wake flow condition. These curves were obtained from data in references 6 and 7. Also shown in this figure is the reentry portion of the flight, with the period of X-band signal loss indicated. The X-band signal-loss period lies in a region that is bracketed by the curves of both X-band blackout prediction theories. This condition indicates a strong possibility that momentary loss of the X-band signal could have been due to radiofrequency blackout by a plasma.

However, this signal-loss period occurred during a time of rapid deceleration of the payload and created a tracking problem for the X-band receiving station (station 2) which was slaved to the S-band radar tracker. The antenna beam width of the S-band tracking radar was twice that of the X-band receiving station. Thus, when the payload reentered the earth's atmosphere and went into the rapid deceleration phase, the S-band tracker could have tended to get ahead of the payload for a few seconds, causing the X-band receiving-station antenna to move off target. This condition occurred during two later flights of Trailblazer II vehicles which were flown for the Air Force Avionics Laboratory with similar X-band systems. These occurrences were at the same approximate flight time, which indicates that tracking error also was a possible cause of the X-band signal loss on the test flight.

CONCLUDING REMARKS

The concept of using a telemetry radiofrequency higher than the critical frequency of the plasma to provide transmission of data during the reentry period has been investigated by use of an X-band telemetry system on a Trailblazer II flight. Although usable signal was lost for a period of about 2.4 seconds during the reentry period, this represents only about one-fourth of the expected signal-loss period due to radiofrequency



blackout for a VHF telemetry system. The loss of the X-band signal during this short period of time was most probably due to either radiofrequency blackout or tracking error.

Postflight simulation tests indicate that the 17-dB reduction in transmitter output power which occurred during the flight could have been caused by a partial failure of the magnetron power supply.

This reduction of output power combined with the modulation of the antenna radiation pattern by vehicle precession resulted in periodic interruption of the received pulse train. These interruptions precluded the use of automatic data-reduction equipment and necessitated manual data reduction. This experience reemphasizes the importance of adequate signal margins for pulse-telemetry systems.

Langley Research Center,
National Aeronautics and Space Administration,
Langley Station, Hampton, Va., September 1, 1967,
125-21-02-07-23.

REFERENCES

1. Huber, Paul W.; and Nelson, Clifford H.: Plasma Frequency and Radio Attenuation. Proceedings of the NASA-University Conference on the Science and Technology of Space Exploration, Vol. 2, NASA SP-11, 1962, pp. 347-360. (Also available as NASA SP-25.)
2. Lundstrom, Reginald R.; Henning, Allen B.; and Hook, W. Ray: Description and Performance of Three Trailblazer II Reentry Research Vehicles. NASA TN D-1866, 1964.
3. Harrington, R. F.; Brummer, E. A.; and Southall, W. A.: A 3-Pound, 1,000-Watt X-Band Reentry Telemetry System. NASA paper presented at 1963 National Space Electronics Symposium (Miami), Oct. 1-3, 1963.
4. Croswell, William F.; and Higgins, Robert B.: Effects of Dielectric Covers Over Shunt Slots in a Waveguide. NASA TN D-2518, 1964.
5. Brummer, E. A.; and Harrington, R. F.: A Unique Approach to an X-Band Telemetry Receiving System. Paper 4-2 of Proceedings of the 1962 National Telemetering Conference, Vol. 1, May 1962. (Sponsored by ARS, AIEE, IAS, ISA, and IRE.)
6. Huber, Paul W.; and Sims, Theo E.: The Entry-Communications Problem. Astronaut. Aeron., vol. 2, no. 10, Oct. 1964, pp. 30-40.
7. Huber, Paul W.: Hypersonic Shock-Heated Flow Parameters For Velocities to 46,000 Feet Per Second and Altitudes to 323,000 Feet. NASA TR R-163, 1963.

TABLE I.- TELEMETRY CHANNELS

Channel	Measurement	Range
1	Battery monitor	0 to 40 V
2	Thermocouple on fourth-stage-motor nozzle	$\begin{cases} 0 \text{ to } 1000^{\circ} \text{ F} \\ -17.8^{\circ} \text{ to } 537.8^{\circ} \text{ C} \end{cases}$
3	Thermocouple on fourth-stage motor	$\begin{cases} 0 \text{ to } 1000^{\circ} \text{ F} \\ -17.8^{\circ} \text{ to } 537.8^{\circ} \text{ C} \end{cases}$
4	Antenna radiofrequency power monitor	0 to 100 W
5	Thermistor on antenna-power monitor	$\begin{cases} 0 \text{ to } 200^{\circ} \text{ F} \\ -17.8^{\circ} \text{ to } 93.3^{\circ} \text{ C} \end{cases}$
6	Thermistor on transmitter face plate	$\begin{cases} 0 \text{ to } 200^{\circ} \text{ F} \\ -17.8^{\circ} \text{ to } 93.3^{\circ} \text{ C} \end{cases}$
7	Accelerometer	$\begin{cases} \pm 100\text{g} \\ \pm 980.7 \text{ m/sec}^2 \end{cases}$
8	Full-scale calibration	20 mV
9	Zero-scale calibration	0 mV
10	Light sensor	0.8 to 80 W/cm ²
11	Light sensor	80 to 1600 W/cm ²
12	Light sensor	0.4 to 40 W/cm ²
13	Light sensor	40 to 80 W/cm ²
14	Thermocouple on tip of nose cone	$\begin{cases} 0 \text{ to } 2000^{\circ} \text{ F} \\ -17.8^{\circ} \text{ to } 1093.3^{\circ} \text{ C} \end{cases}$
15	Thermocouple on light sensor	$\begin{cases} 0 \text{ to } 200^{\circ} \text{ F} \\ -17.8^{\circ} \text{ to } 93.3^{\circ} \text{ C} \end{cases}$
16	Thermocouple on nose cone	$\begin{cases} 0 \text{ to } 2000^{\circ} \text{ F} \\ -17.8^{\circ} \text{ to } 1093.3^{\circ} \text{ C} \end{cases}$
17	Blank channel	
18	Blank channel	
19	Frame synchronization	
20	Frame synchronization	

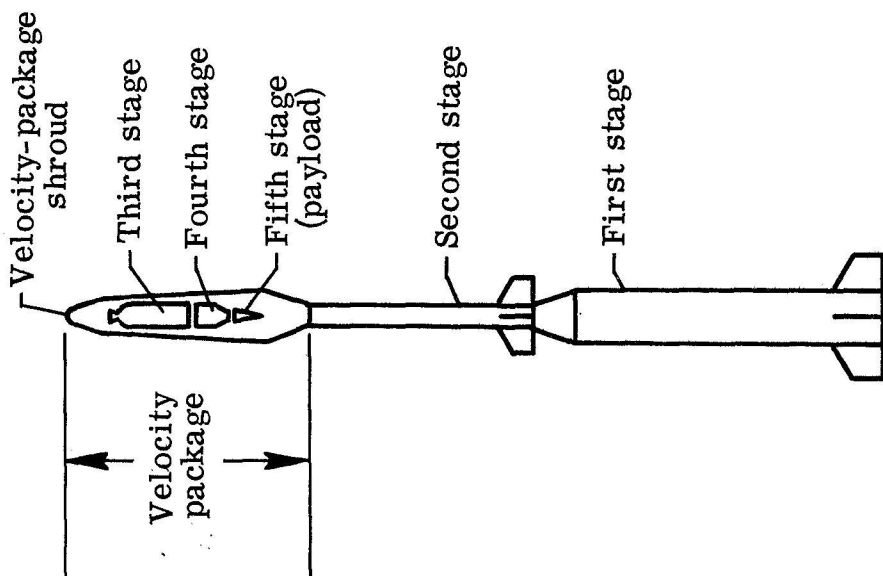
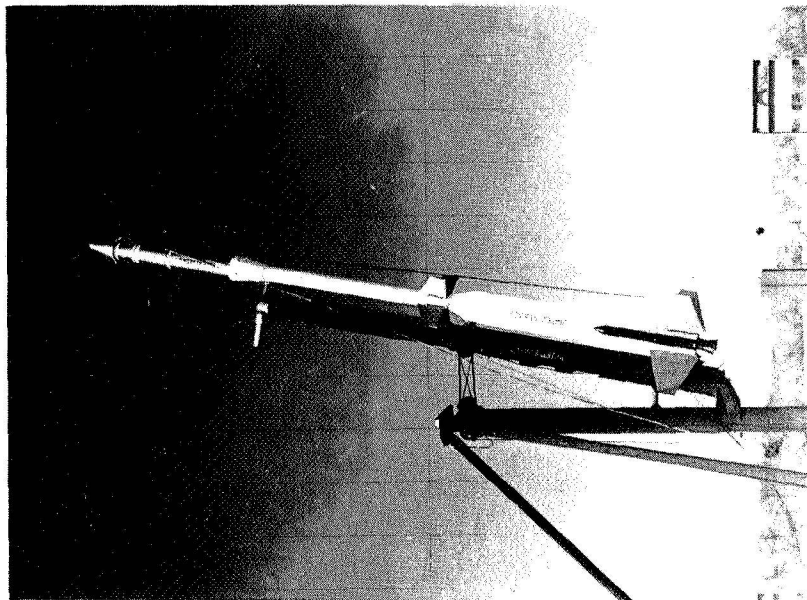


Figure 1.- Five-stage Trailblazer II reentry-research vehicle.

L-67-6670

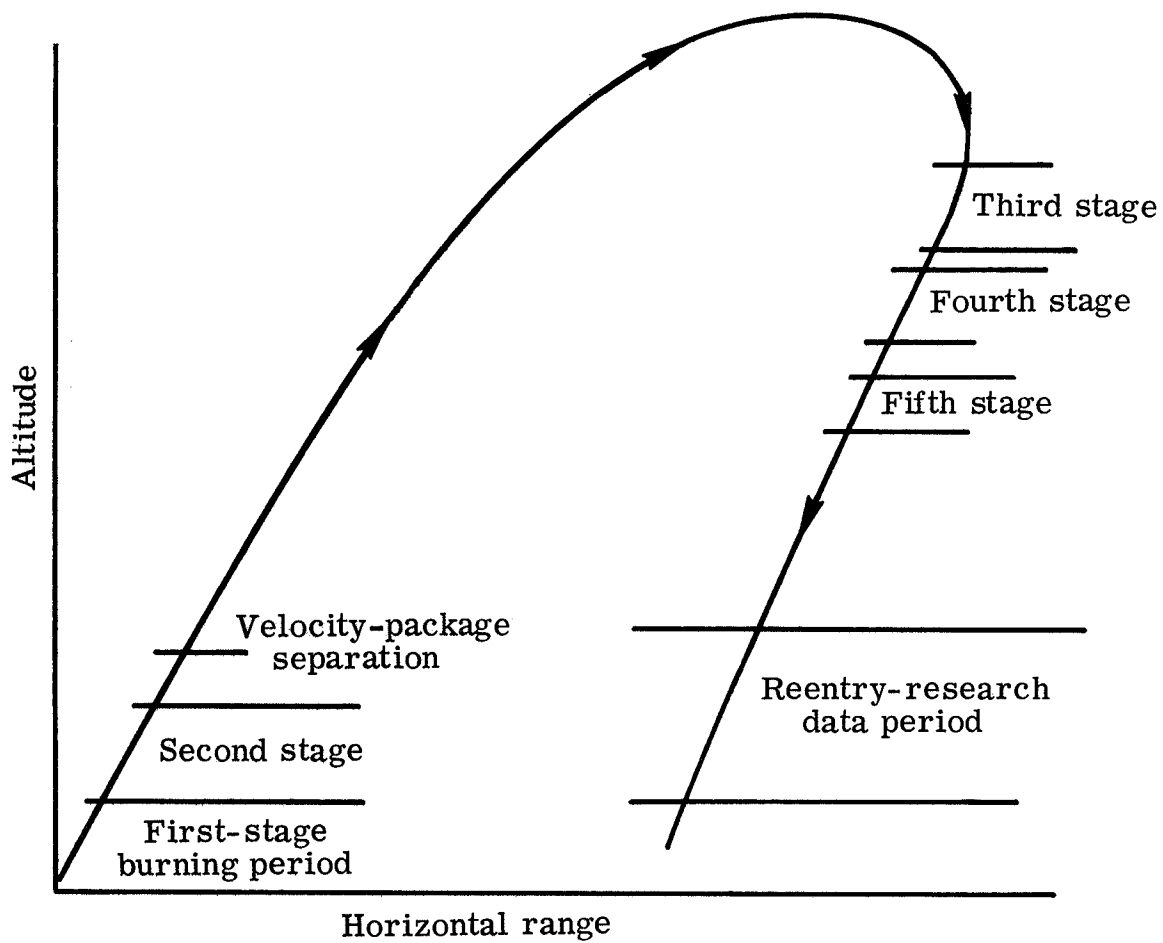


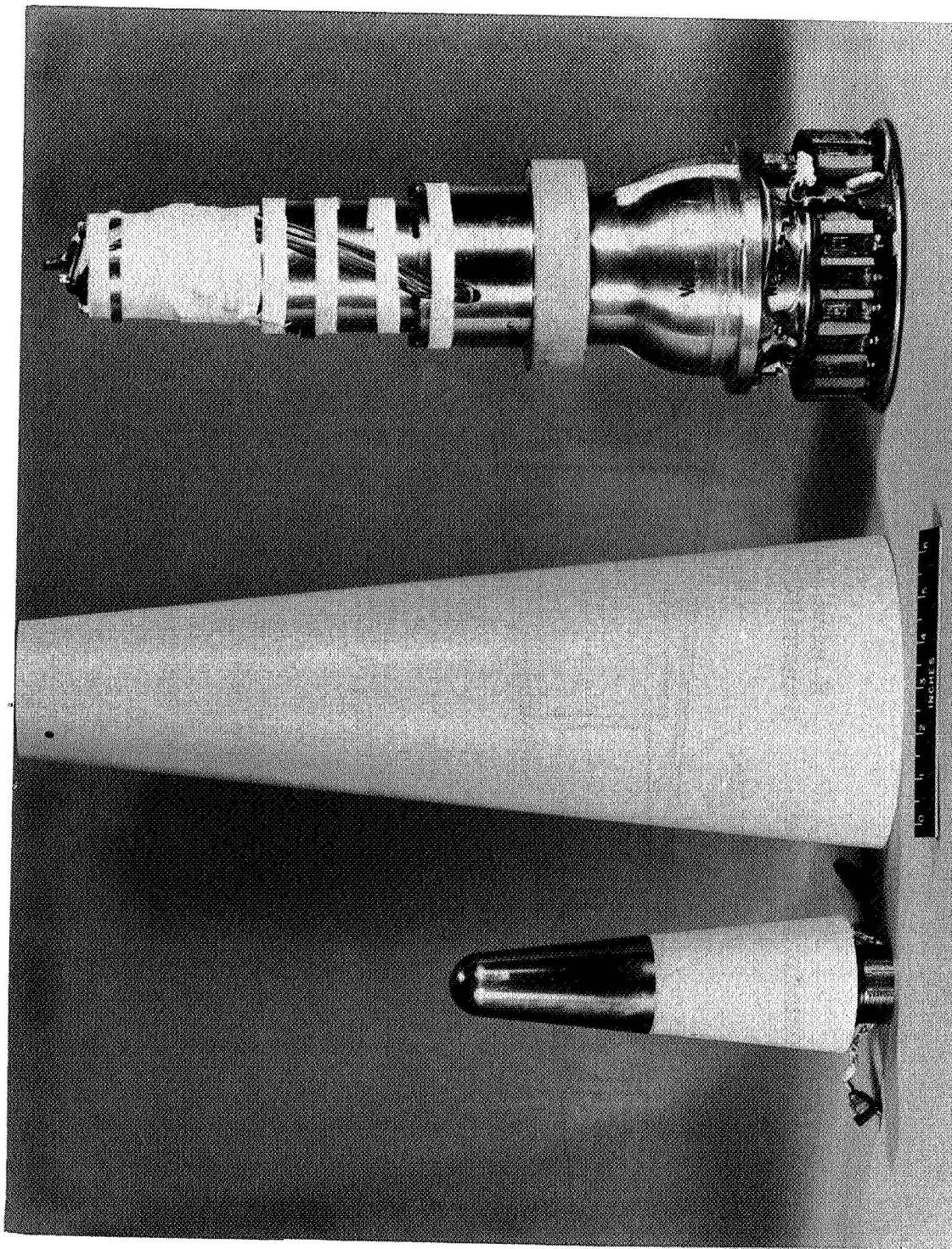
Figure 2.- Trailblazer II trajectory.



(a) Photograph of assembled payload.

L-63-8298

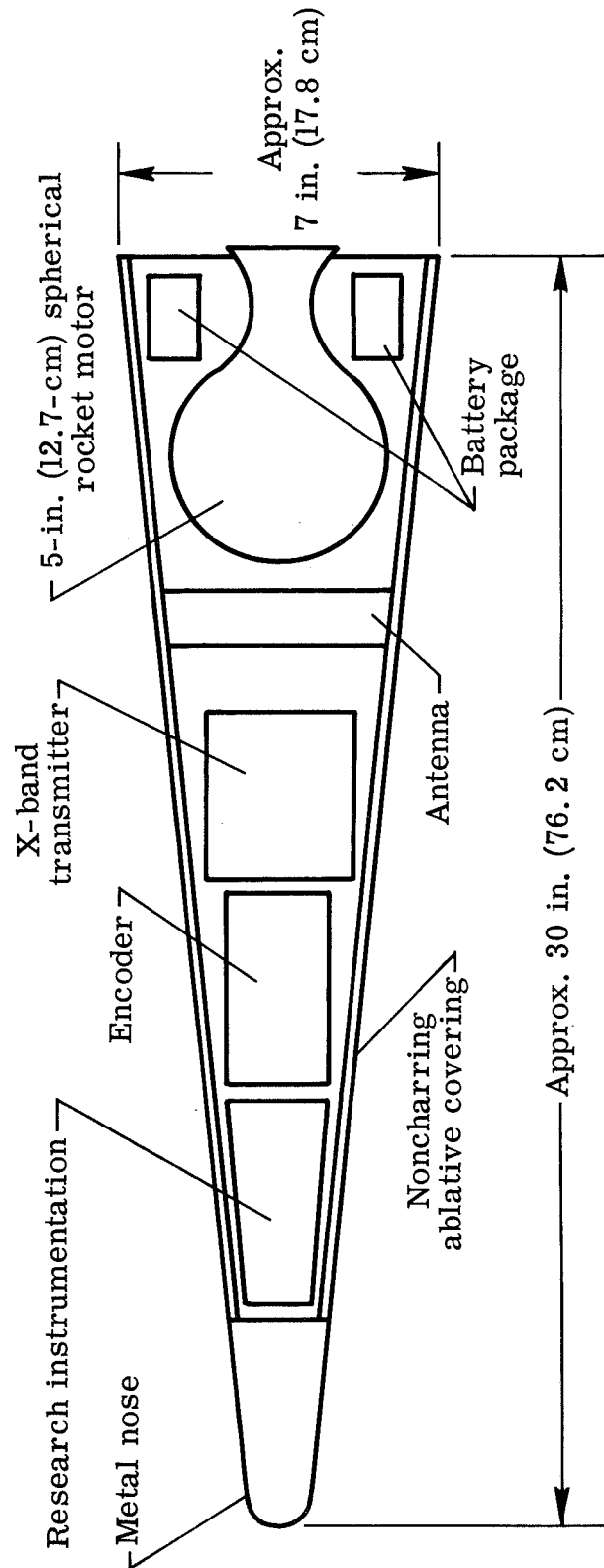
Figure 3.- Trailblazer II payload.



(b) Photograph of unassembled payload.

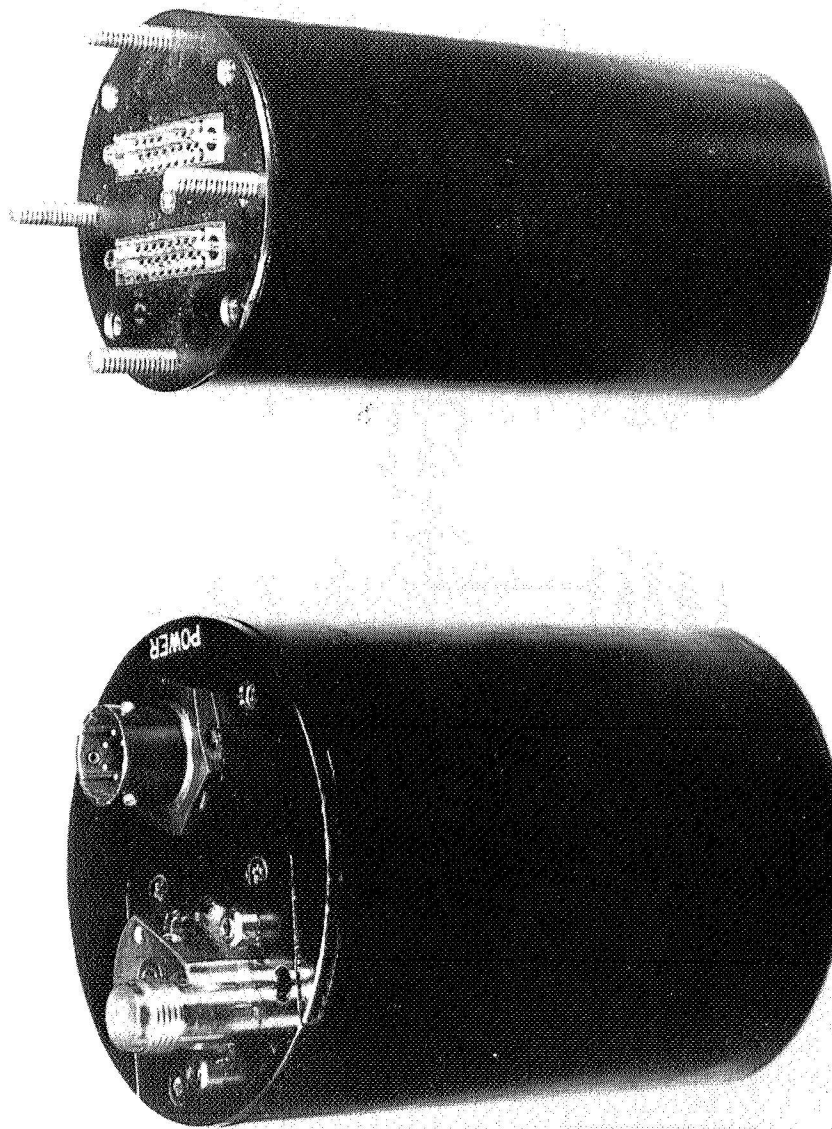
Figure 3.- Continued.

L-63-8299



(c) Payload configuration.

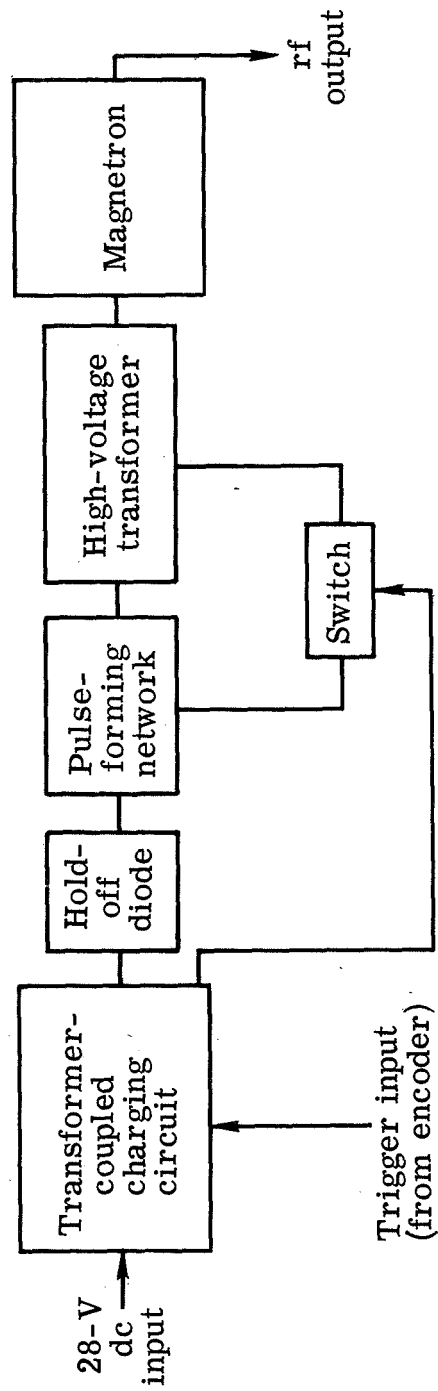
Figure 3.- Concluded.



(a) Photograph of transmitter and encoder.

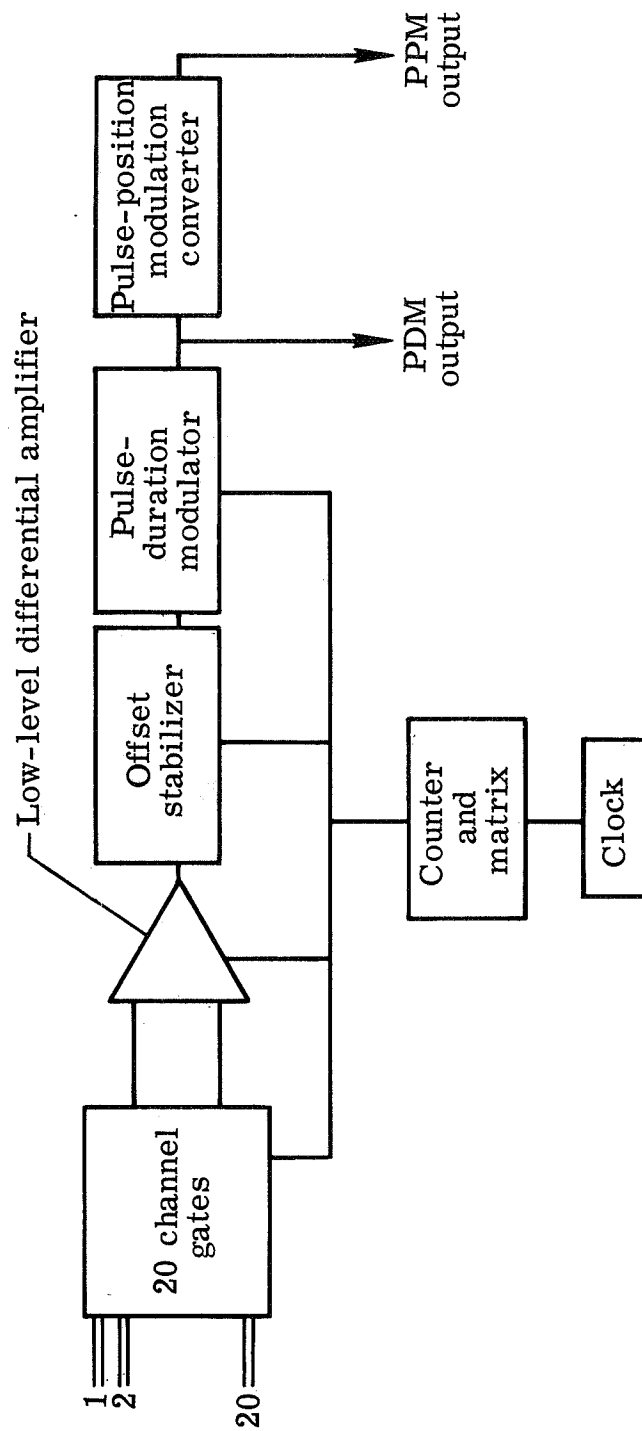
Figure 4.- X-band transmitter and encoder.

L-67-6672



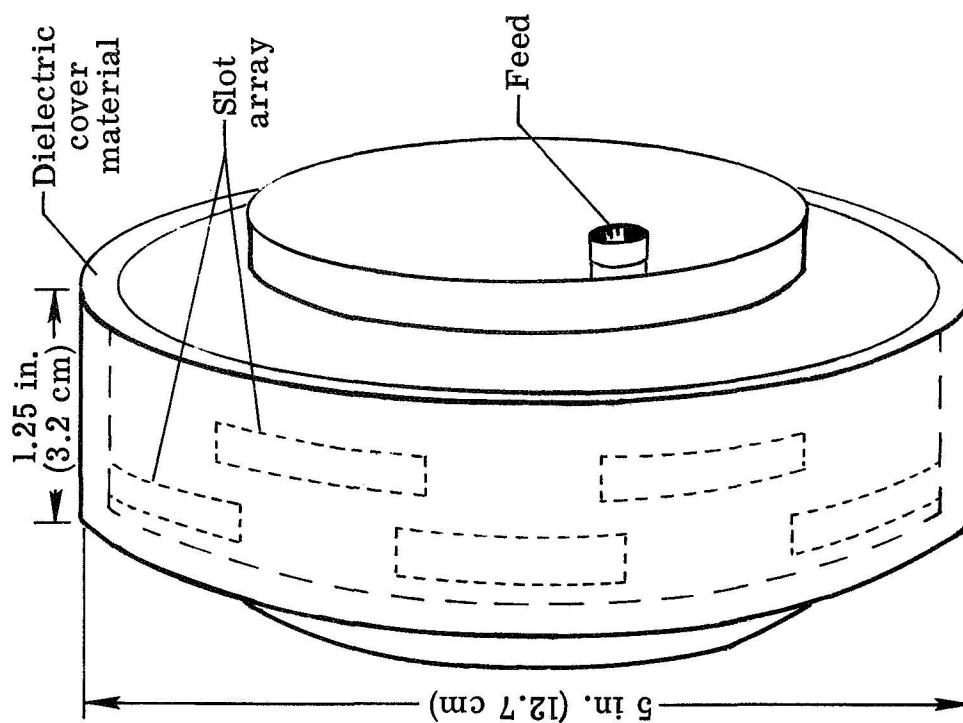
(b) Simplified block diagram of transmitter.

Figure 4.- Continued.



(c) Simplified block diagram of encoder.

Figure 4.- Concluded.

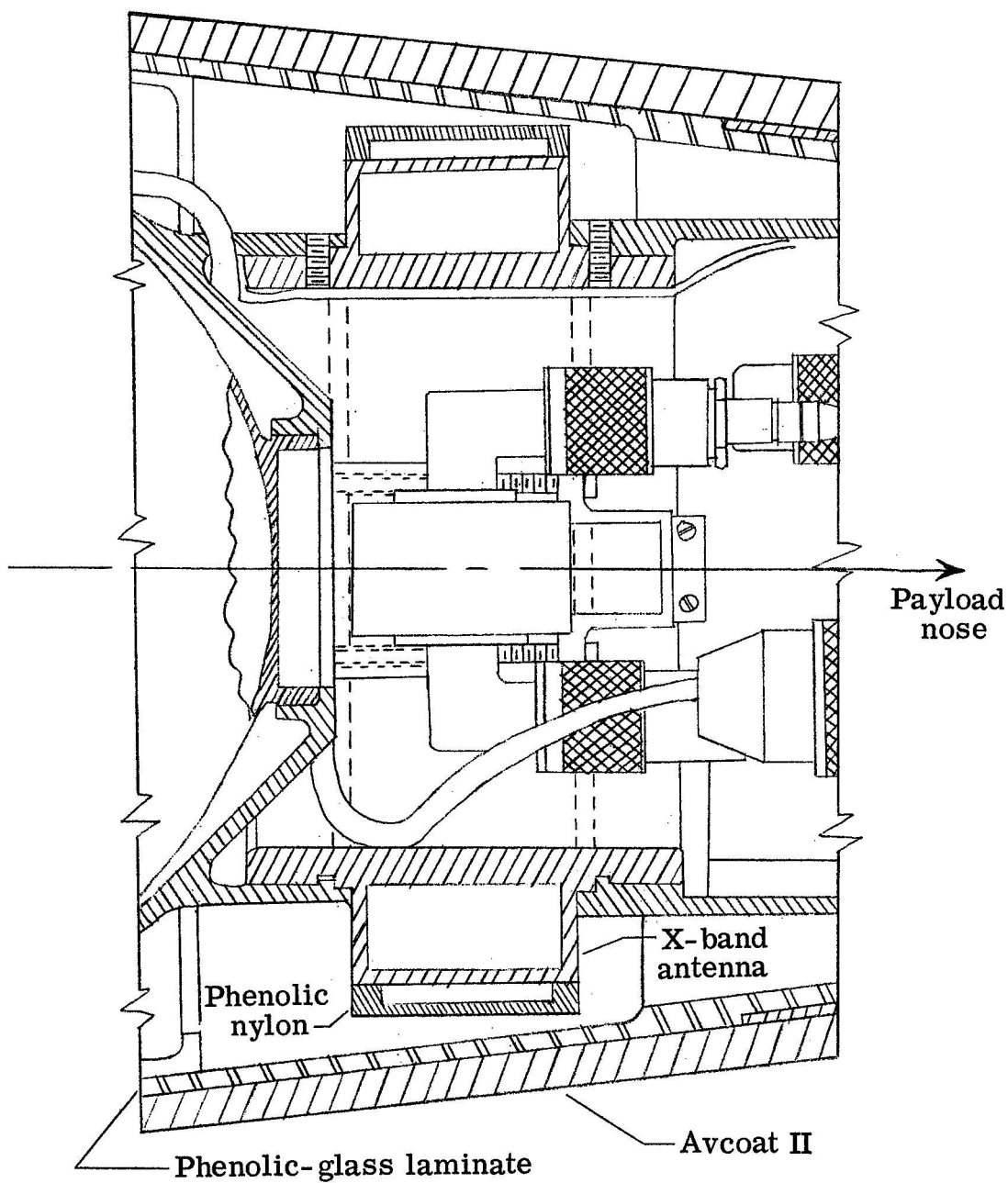


L-67-6671



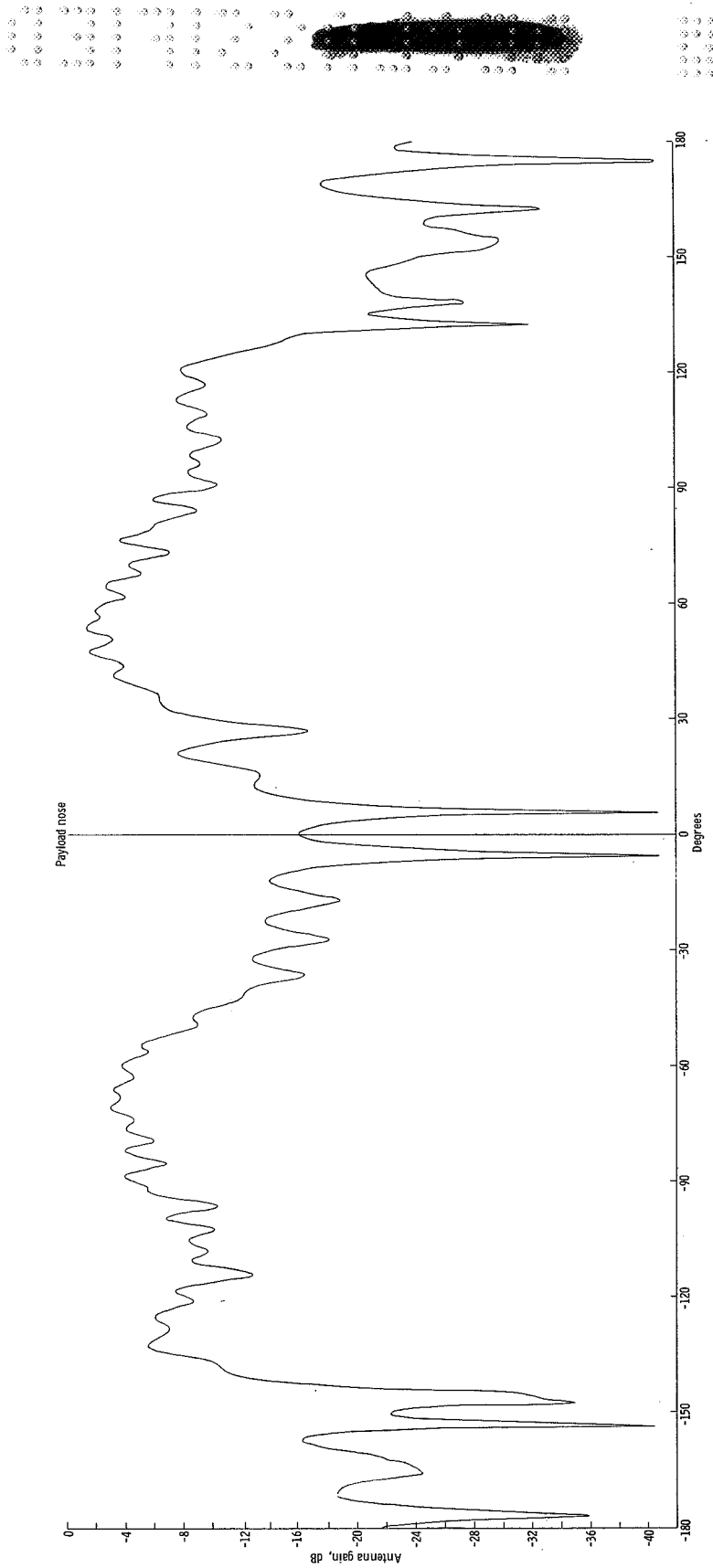
(a) Photograph and configuration of antenna.

Figure 5.- Slot array X-band payload antenna.



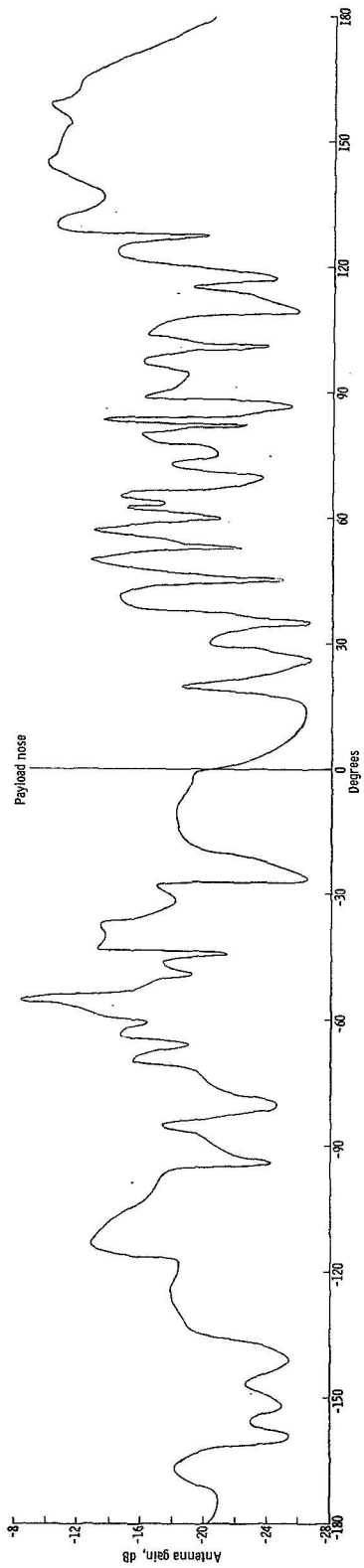
(b) Sectional view of X-band antenna mounted in Trailblazer II payload.

Figure 5.- Concluded.

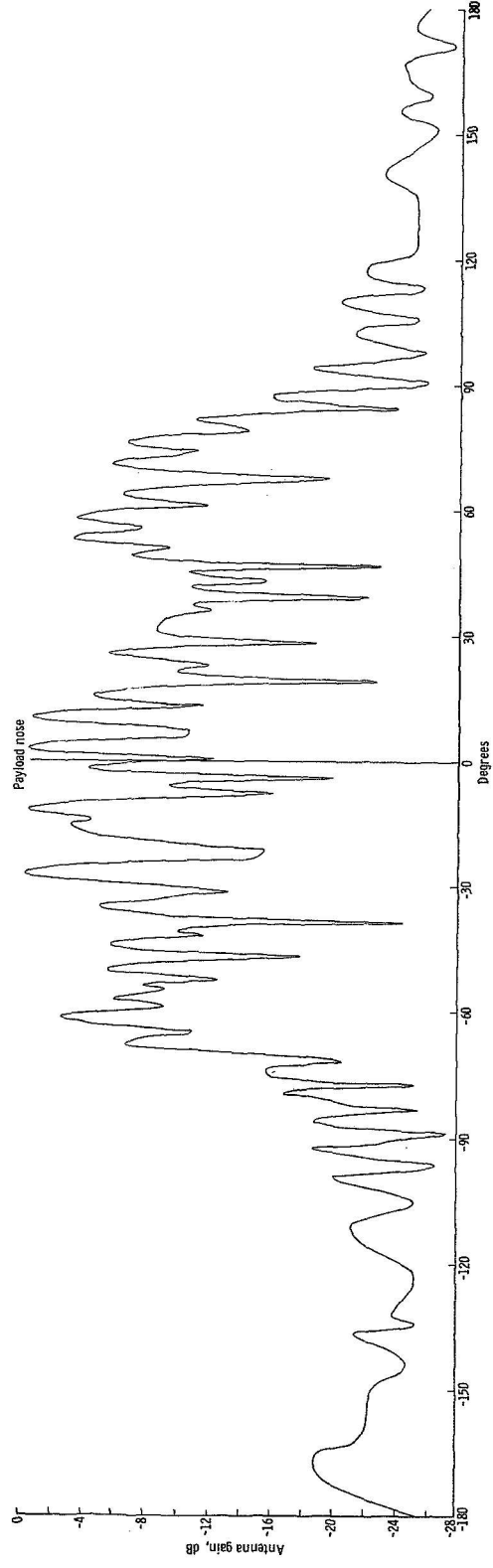


(a) Pitch-yaw plane radiation pattern for payload.

Figure 6.- X-band antenna radiation patterns.



(b) Pitch-yaw plane radiation pattern for closed velocity shroud.



(c) Pitch-yaw plane radiation pattern for open-end velocity shroud.

Figure 6.- Concluded.

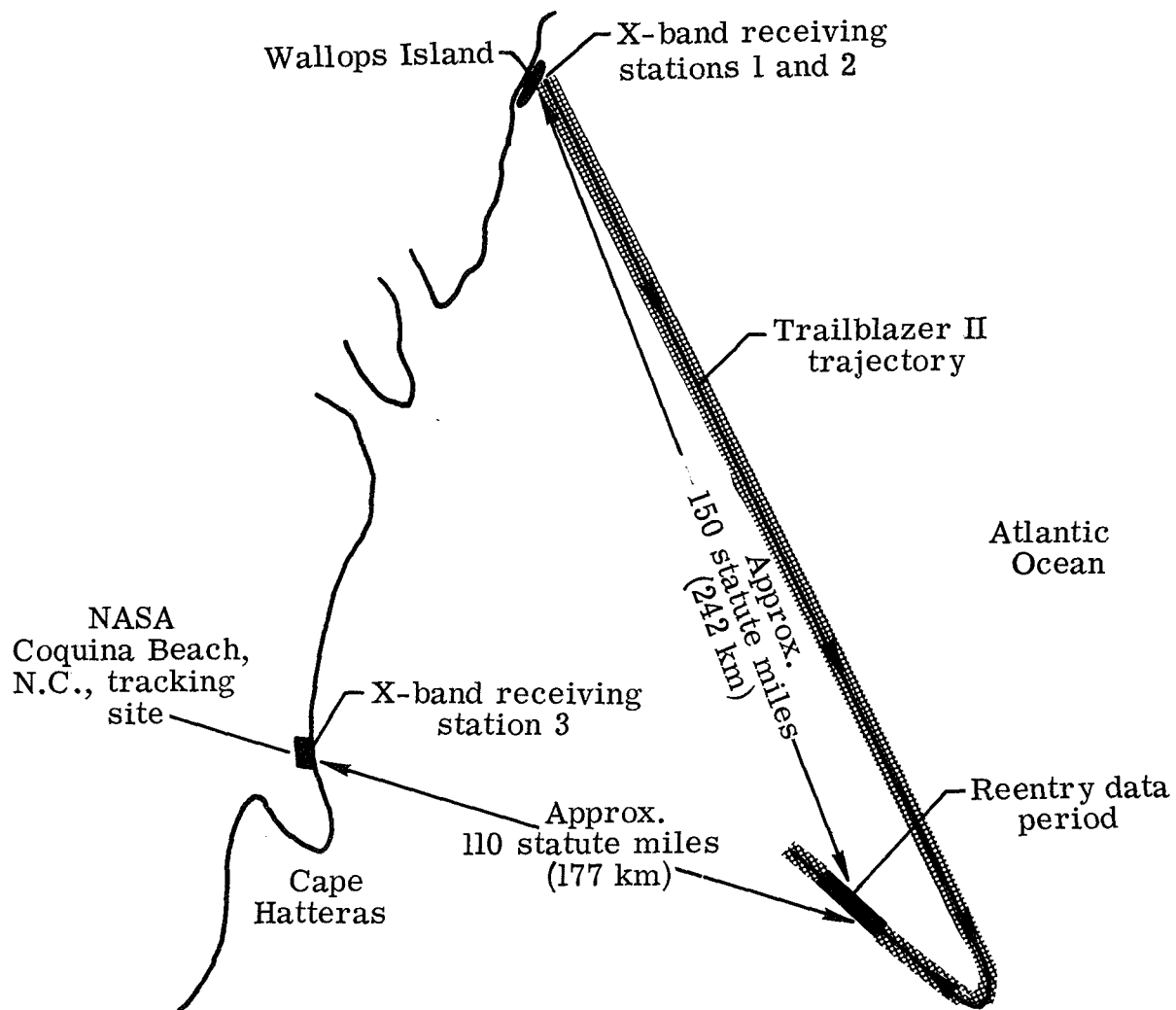


Figure 7.- Trailblazer II trajectory plan view.

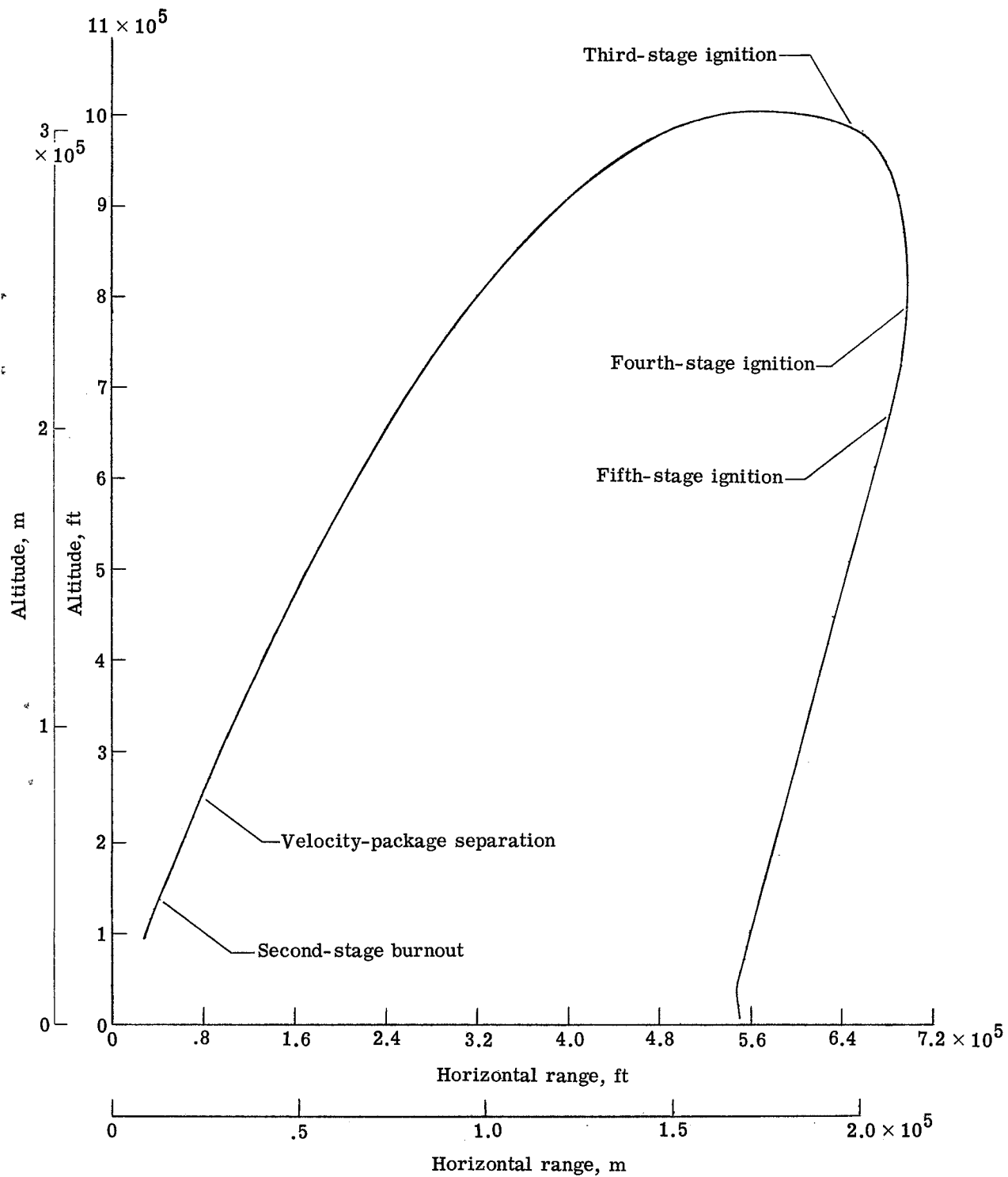


Figure 8.- Flight path of D58-3539 Trailblazer II.

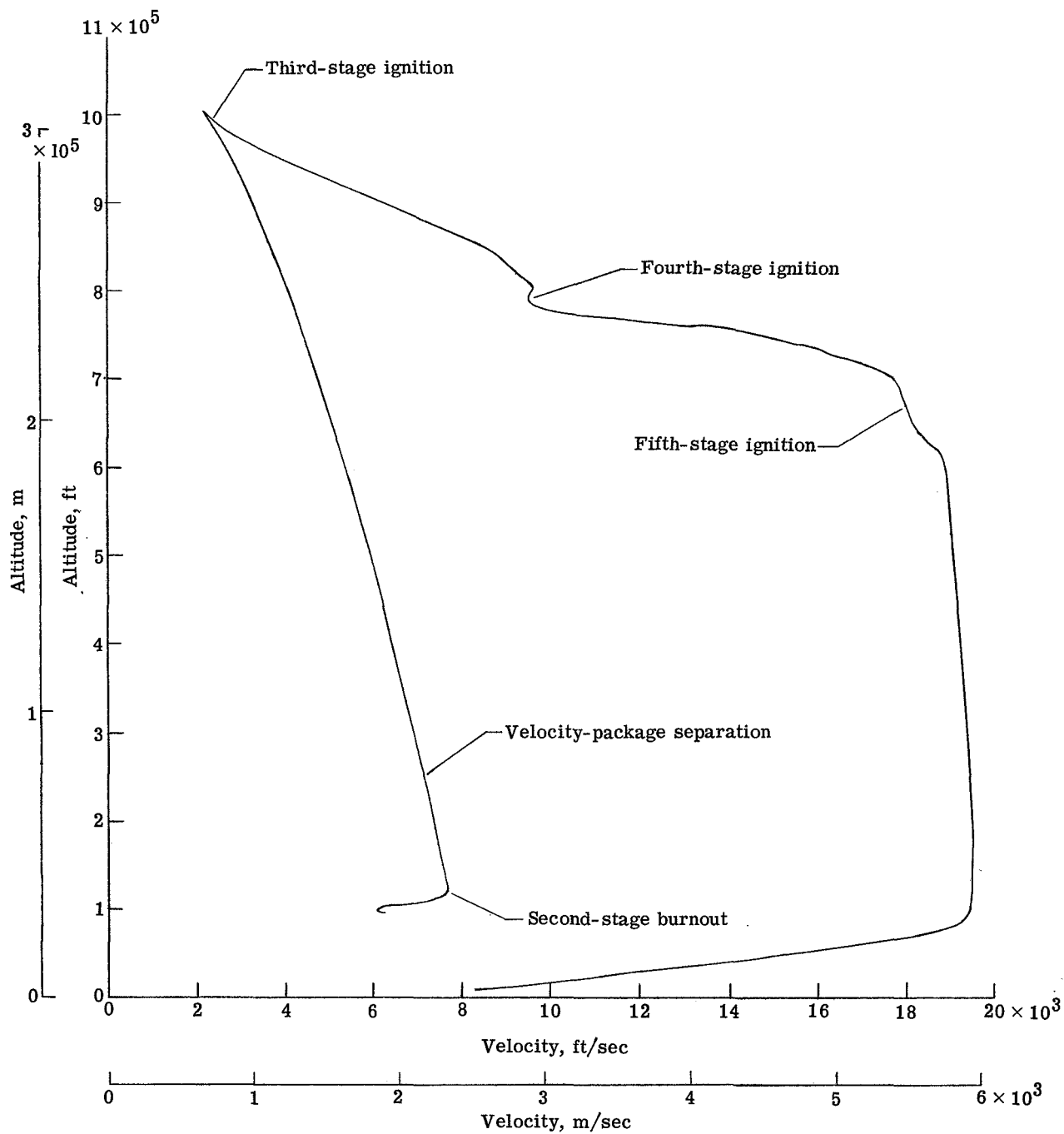


Figure 9.- Altitude-velocity profile of D58-3539 Trailblazer II.

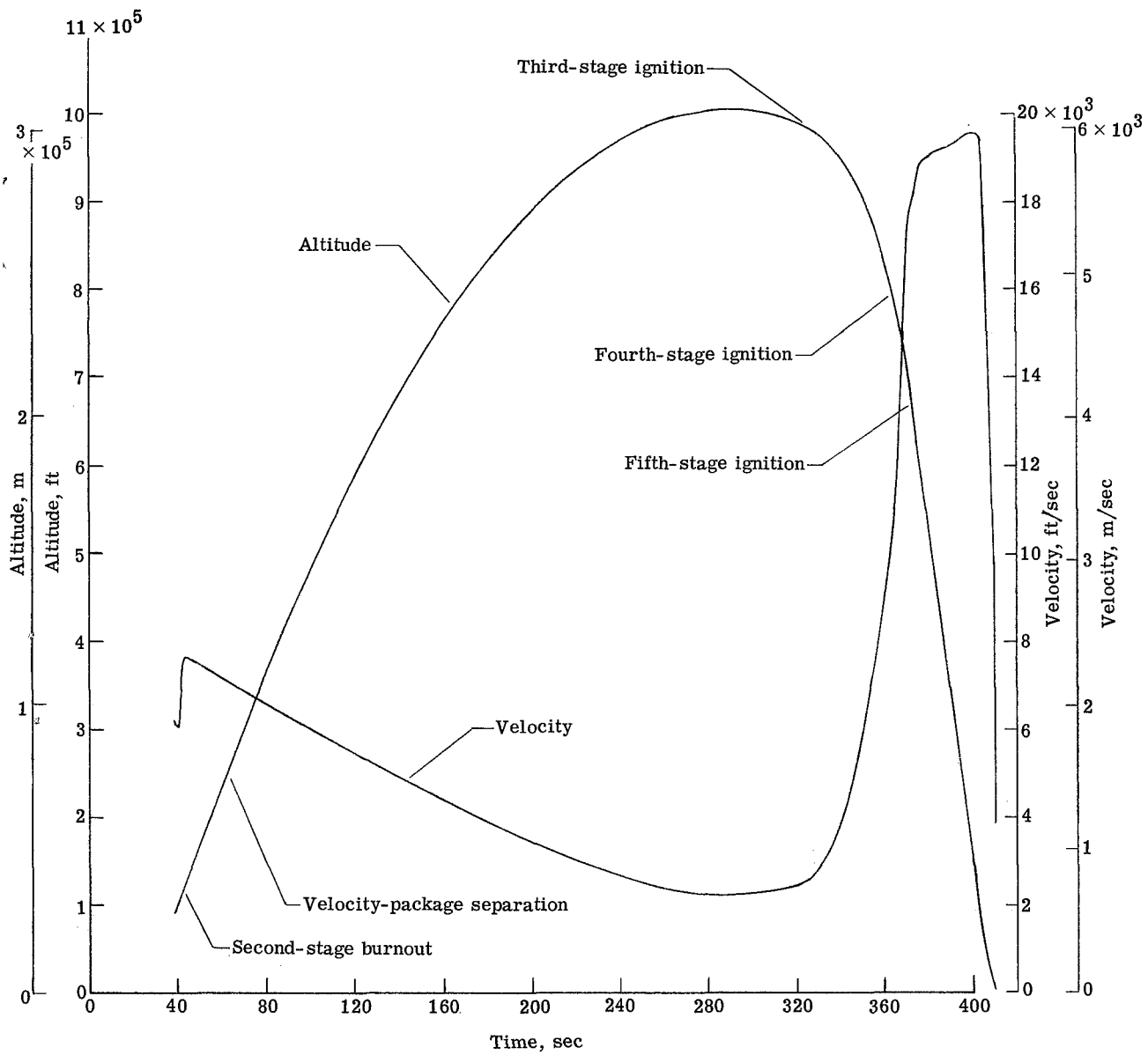


Figure 10.- Altitude and velocity time histories of D58-3539 Trailblazer II.

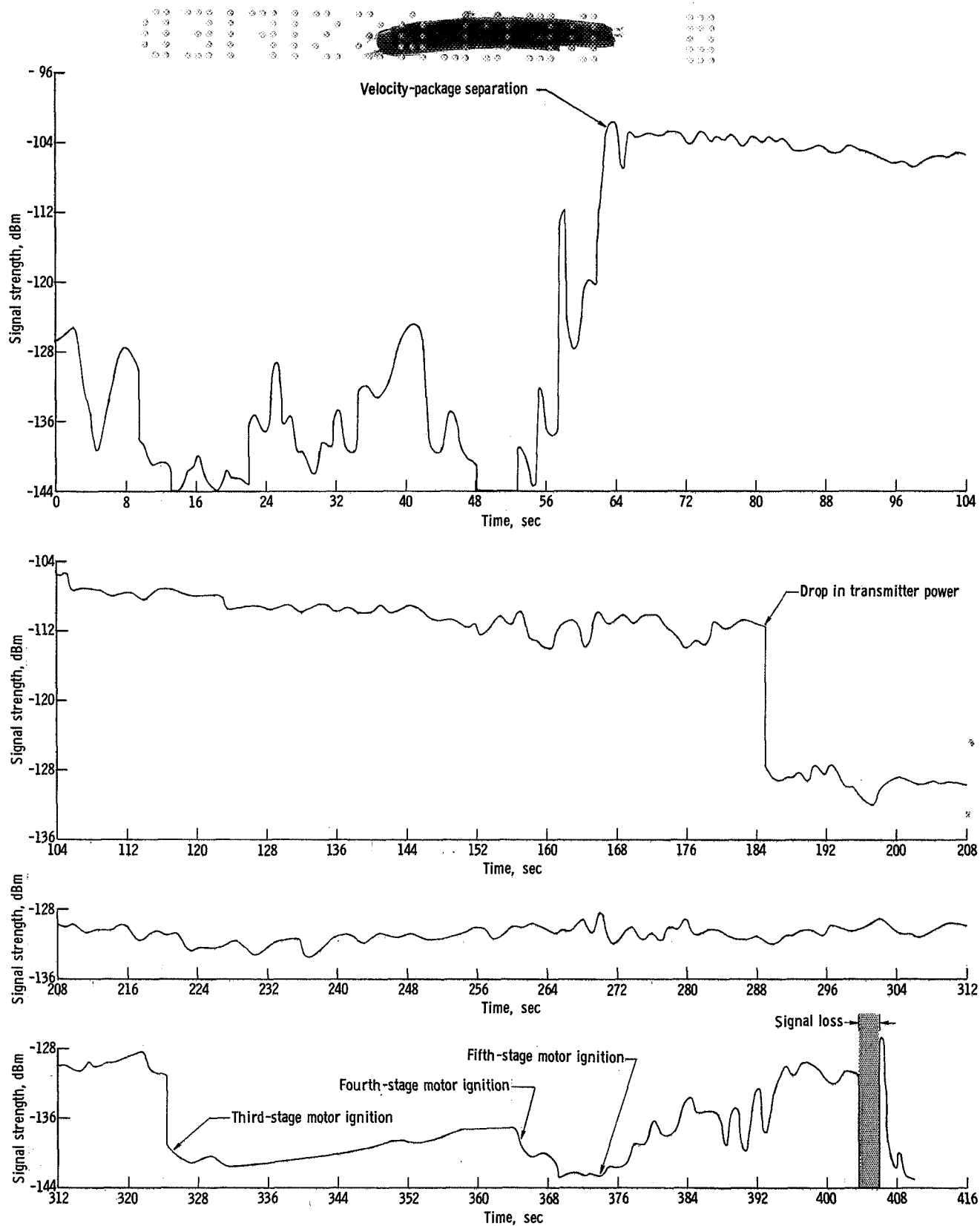


Figure 11.- Received X-band signal strength at the antenna of the M.I.T. tracking station.

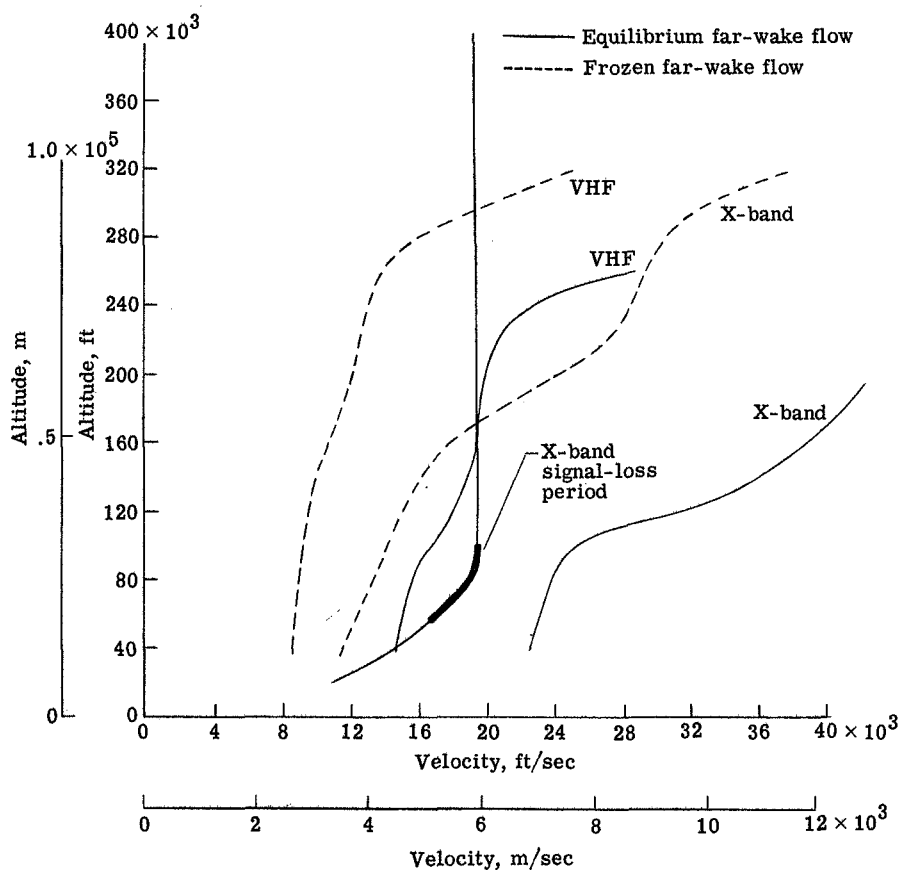


Figure 12.- Velocity-altitude profile showing predicted VHF and X-band blackout areas and observed X-band signal-loss period during the reentry portion of the flight.



"The aeronautical and space activities of the United States shall be conducted so as to contribute . . . to the expansion of human knowledge of phenomena in the atmosphere and space. The Administration shall provide for the widest practicable and appropriate dissemination of information concerning its activities and the results thereof."

—NATIONAL AERONAUTICS AND SPACE ACT OF 1958

NASA SCIENTIFIC AND TECHNICAL PUBLICATIONS

TECHNICAL REPORTS: Scientific and technical information considered important, complete, and a lasting contribution to existing knowledge.

TECHNICAL NOTES: Information less broad in scope but nevertheless of importance as a contribution to existing knowledge.

TECHNICAL MEMORANDUMS: Information receiving limited distribution because of preliminary data, security classification, or other reasons.

CONTRACTOR REPORTS: Scientific and technical information generated under a NASA contract or grant and considered an important contribution to existing knowledge.

TECHNICAL TRANSLATIONS: Information published in a foreign language considered to merit NASA distribution in English.

SPECIAL PUBLICATIONS: Information derived from or of value to NASA activities. Publications include conference proceedings, monographs, data compilations, handbooks, sourcebooks, and special bibliographies.

TECHNOLOGY UTILIZATION PUBLICATIONS: Information on technology used by NASA that may be of particular interest in commercial and other non-aerospace applications. Publications include Tech Briefs, Technology Utilization Reports and Notes, and Technology Surveys.

Details on the availability of these publications may be obtained from:

SCIENTIFIC AND TECHNICAL INFORMATION DIVISION
NATIONAL AERONAUTICS AND SPACE ADMINISTRATION

Washington, D.C. 20546